THE JOURNAL OF PHYSICAL CHEMISTRY C

Article

pubs.acs.org/JPCC

Determination of the Nature of the Cu Coordination Complexes Formed in the Presence of NO and NH_3 within SSZ-13

Ines Lezcano-Gonzalez,[†,‡] David S. Wragg,[§] Wojciech A. Slawinski,[§] Karen Hemelsoet,[∥] Andy Van Yperen-De Deyne,[∥] Michel Waroquier,[∥] Veronique Van Speybroeck,[∥] and Andrew M. Beale*[,†,‡]

[†]Department of Chemistry, University College London, 20 Gordon Street, London WC1H 0AJ, U.K.

[‡]UK Catalysis Hub, Research Complex at Harwell, Rutherford Appleton Laboratory, Didcot OX11 0FA, U.K.

[§]INGAP Centre for Research Based Innovation, Department of Chemistry, University of Oslo, Oslo N-0315, Norway

[∥]Center for Molecular Modelling (CMM), Ghent University, Technologiepark 903, Zwijnaarde B-9052, Belgium

Supporting Information

ABSTRACT: Ammonia-selective catalytic reduction (NH_3-SCR) using Cu zeolites is a well-established strategy for the abatement of NO_x gases. Recent studies have demonstrated that Cu is particularly active when exchanged into the SSZ-13 zeolite, and its location in either the *6r* or *8r* renders it an excellent model system for fundamental studies. In this work, we examine the interaction of NH_3-SCR relevant gases (NO and NH_3) with the Cu^{2+} centers within the SSZ-13 structure, coupling powder diffraction (PD), X-ray absorption spectroscopy (XAFS), and density functional theory (DFT). This combined approach revealed that, upon calcination, cooling and gas exposure Cu ions tend to locate in the *8r* window. After NO introduction, Cu ions are seen to coordinate to two framework oxygens and one NO molecule, resulting in a bent Cu−nitrosyl complex with a Cu−N−O bond angle of ∼150°. Whilst Cu seems to be partially reduced/changed in coordination state, NO is partially oxidized. On exposure to NH_3 while the PD data suggest the Cu^{2+} ion occupies a similar position, simulation and XAFS pointed toward the formation of a Jahn−Teller distorted hexaamine complex $[Cu(NH_3)_6]^{2+}$ in the center of the *cha* cage. These results have important implications in terms of uptake and storage of these reactive gases and potentially for the mechanisms involved in the NH_3-SCR process.

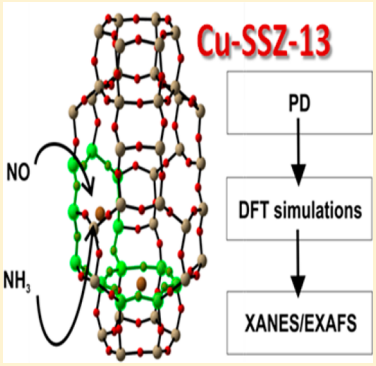

1. INTRODUCTION

Ammonia-selective catalytic reduction (NH_3-SCR) using zeolites is a well-established technology to remove NO_x compounds from oxygen-rich exhausts, characteristic of diesel engines.[1−3] Since the initial studies by Iwamoto et al. and Konig et al.,[4,5] many zeolites of varying topology containing different transition metal ion (TMI) components have been tested in the NH_3-SCR reaction, with Cu-containing zeolites exhibiting a very high activity and selectivity over a wide temperature window. In particular, the superior activity and enhanced hydrothermal stability of Cu-exchanged SSZ-13 zeolite, based on the CHA topology, have led to its commercialization for mobile applications.[1−3]

Over the past few years many characterization methods have been applied to gain insight into the exceptional catalytic performance of Cu-SSZ-13 zeolite investigating, among other aspects, the nature and location of the Cu active sites.[6−13] Initial studies indicated that Cu^{2+} ions occupy positions in the *6r* of the primary *d6r* structures of SSZ-13 zeolite,[6−8] in agreement with density functional theory (DFT) calculations, which showed a better stability for Cu^{2+} ions in this configuration.[14,15] Subsequent works, however, reported an effect of Cu loading on Cu location; i.e., at low Cu loadings, Cu^{2+} ions are located in the *6r*, whereas at higher loadings, Cu^{2+} ions occupy positions in both the *6r* and *8r*.[9,10] The preference for Cu to reside in the *8r* has been recently supported by Rietveld/maximum entropy methods applied to synchrotron powder XRD data in combination with DFT calculations[11] as well as EXAFS analysis combined with X-ray absorption near edge structure/X-ray emission spectroscopy (XANES/XES) simulations of a high-loaded Cu-SSZ-13 sample,[12] evidencing that the majority of Cu species are located at a specific site in the *8r* under dehydrated conditions. Interestingly, it has been anticipated that isolated Cu^{2+} ions may migrate within the SSZ-13 structure during dehydration or else interaction with adsorbates, suggesting a more complicated picture for the location of the active Cu species in SSZ-13.[13]

Besides the nature and location of the active Cu sites, the SCR reaction mechanism has been controversial until now.[1−3] Several studies have been performed to determine the intermediate species formed upon NO or NH_3 adsorption on Cu-SSZ-13 zeolite and their participation in the SCR reaction.

Received: July 16, 2015
Revised: September 25, 2015
Published: October 1, 2015

DOI: 10.1021/acs.jpcc.5b06875
J. Phys. Chem. C 2015, 119, 24393−24403

FTIR and ^{15}N MAS NMR studies provided evidence of the formation of side-on $Cu^{+}\cdots NO^{+}$ species upon NO adsorption on Cu-SSZ-13, produced by direct oxidation of NO over Cu^{2+} or by NO_2 disproportionation.[1,3,16] The optimized geometry showed a Cu−N−O angle of 146.7°. These results were in line with earlier IR data, which showed the formation of nitrosyl species on Cu-SSZ-13.[1,3,17] Accordingly, a reaction mechanism was anticipated, wherein the initially formed $Cu^{+}\cdots NO^{+}$ intermediates react with water, forming $Cu^{+}HONO/H^{+}$ species that convert, in turn, into ammonium nitrite-like complexes by reaction with NH_3. N_2 and water are then formed from the decomposition of ammonium nitrite-like complexes.[16] In contrast, on the basis of operando XAS and DFT data, it has been proposed the formation of $Cu^{+}H_2NNO/H^{+}$ intermediate species from NO-assisted dissociation of NH_3 bounded to Cu^{2+} sites.[18] These species decompose to N_2 and water, which are also produced in subsequent steps of the mechanism from the decomposition of adjacent NO_2^{-} and NH_4^{+} ions adsorbed on Cu^{2+} sites.[18] Very recently, a complete catalytic cycle of the NH_3-SCR reaction has been reported, in which the standard SCR is a combination of NO oxidation with the fast SCR reaction (i.e., NO is proposed to react with surface nitrate species, leading to the release of one NO_2 molecule and leaving a nitrite species at the metal site). Overall, the reaction is shown to proceed via two general steps, oxidation of the catalyst by NO + O_2 and reduction by NO + NH_3, being the oxidation of NO by O_2 to form bidentate nitrates the rate-determining step for standard SCR.[19]

Similarly, the nature and role of NH_3 adsorbed species have also been extensively investigated. Earlier *in situ* XAS/XRD studies revealed a change in the local geometry of Cu at low temperatures (from square planar to tetrahedral) due to the direct interaction with one NH_3 molecule, coinciding with a low catalytic activity. Notably this process was seen to be reversible at temperatures typical of maximum activity and therefore related to a blocking interaction of NH_3 at low temperatures.[8] Subsequent DFT calculations combined with *in situ* FTIR measurements at 250 °C showed the presence of a number of adsorbed species, including NH_4^{+} ions, formed on the Brønsted acid sites, $[Cu(NH_3)_4]^{2+}$ complexes, resulting from NH_3 coordination with the Cu^{2+} Lewis sites, and NH_3 adsorbed on extra-framework Al (EFAl) species.[20] The NH_4^{+} ions reacted very slowly in comparison to NH_3 coordinated to the Cu^{2+} ions,[20,21] and the Brønsted acid sites were proposed to act mainly as NH_3 storage sites.[20] Later, also based on FTIR results, it was shown the existence of $NH_4^{+}\cdot nNH_3$ associations, while from the combination of DFT calculations and XANES/XES data, it was reported the formation of linear Cu^{+} species in O(framework)−Cu−NH_3 or H_3N−Cu−NH_3 configurations upon NH_3 exposure at 393 K, with an almost linear adsorption geometry in the case of one ammonia molecule, and a N−Cu−N angle of 177° in the case of two ammonia molecules.[22] Nevertheless, whereas *in situ* EPR and NMR combined with DFT indicated that NH_3 leads to Cu^{2+} reduction to Cu^{+}—allowing as well the identification of a variety of Cu−NH_3 complexes and NH_4^{+} ions[23]—combined operando XAS and DFT calculations indicated that NO and NH_3 together are necessary for the reduction of Cu^{2+}.[18] This is in line with very recent results, which showed that exposure to NO alone lead to a Cu^{2+} state, while NH_3 alone lead primarily to a $[Cu(NH_3)_4]^{2+}$ complex.[19]

In this study, Cu-SSZ-13 samples were studied at room temperature using combined X-ray absorption spectroscopy and powder diffraction (XAFS/PD) after exposure to NO or NH_3 so as to be able to investigate both the location of Cu species within the zeolite framework and the interaction between the reactants and the Cu sites (see Figure 1). The

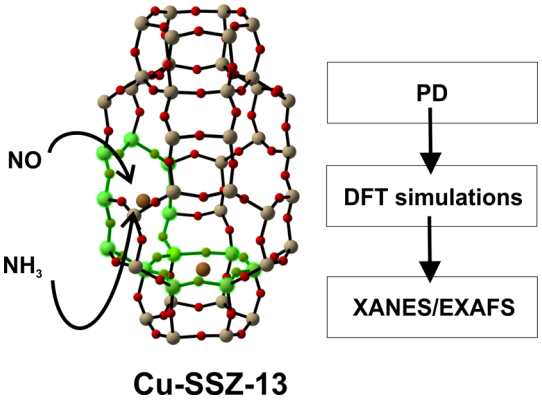

Figure 1. Illustration of the *cha* cage, with *6r* and *8r* indicated in green. Possible locations for the copper sites are shown in brown. The techniques used in the present study to structurally characterize Cu coordination complexes upon interaction with the crucial SCR gases, NO and NH_3, are also given.

advantage in combining these two techniques is that the XAFS data provides local "real space" information regarding the local coordination state around the Cu ion, whereas PD provides the long-range reciprocal space information to observe the vicinity around the Cu species present in a particular location.[8] The strategy employed for analyzing the data involved first determining from PD data a starting model for the distribution/behavior of Cu in the presence of NO or NH_3. On the basis of these results, additional DFT based static and dynamic simulations were performed, so as to come up with more accurate descriptions of the interaction of NO and NH_3 with the Cu species present in SSZ-13. The resultant models were then further optimized using EXAFS in order to account for any local (real-space) differences in the Cu environment.

2. EXPERIMENTAL AND THEORETICAL METHODS

2.1. Catalyst Materials. Details on the synthesis of SSZ-13 (Si/Al = 15) and consequent ion exchange to obtain Cu-SSZ-13 (2 wt % Cu; Si/Al = 15) are mentioned in a previous study and not repeated herein.[20]

2.2. *In Situ* Synchrotron Studies. Separate XAFS and PD measurements were performed at the Swiss-Norwegian beamline (SNBL; BM01B and BM01A, respectively) in the European Synchrotron Research Facility (ESRF), Grenoble, France.[24] SNBL offers a preset gas rig, thereby enabling *in situ* measurements without the need of assembling additional setups. To adapt to the laboratory plug-flow conditions, sieved fractions of samples were packed into quartz capillaries (2 and 0.5 mm diameter, respectively). To study the adsorption behavior of NO and NH_3, the sample was first calcined at 773 K in a 5% O_2/He flow (20 mL/min). This was allowed to cool to room temperature (RT), at which point the gas flow was changed to 10 mL/min of 0.5% NO/He (or 0.5% NH_3/He) and allowed to reach steady state for 10 min before measurements were performed.

2.2.1. X-ray Absorption Fine Structure (XAFS). Using a Si(111) double crystal monochromator, X-ray absorption data at the Cu K-edge (8979 eV) were collected in transmission

DOI: 10.1021/acs.jpcc.5b06875
J. Phys. Chem. C 2015, 119, 24393−24403

mode at RT. Acquisition was performed over several minutes to obtain good statistics (signal-to-noise) for the data collected. The X-ray absorption data were background corrected using Athena (IFFEFIT software package).[25,26] A second-order polynomial was fitted to the raw data in the pre-edge region followed by a cubic spline with k^2-weighting through the post-edge region. The edge jump was defined by extrapolating the spline background to the edge energy (8979 eV) and multiplying the background-subtracted data by a scale factor to give an edge jump of 1.0. The normalized data were k^3-weighed, and a least-squares fitting analysis was performed over a k-range of 3−11 Å^{-1}. The FT of the k^3-weighed data were phase corrected and fit (using single scattering paths) to the proposed theoretical model using the DL-EXCURV program. An amplitude reduction factor (S_0^2) value of 0.9 was used for all data sets.[27] Errors in the determination of the parameters derived from the fitting of the EXAFS data were estimated to be 10% of the coordination number and Debye−Waller factor and ∼0.02 Å for bond distance.[28]

2.2.2. Powder Diffraction (PD). X-ray diffraction data were collected at beamline BM01A of the ESRF (the Swiss-Norwegian beamline). The diffractometer is based on a Huber goniometer with a Pilatus 2 M detector. X-rays with a wavelength of 0.698 11 Å were used, selected by two Rh-coated mirrors and a silicon (111) double crystal monochromator. The beamline setup is described in detail elsewhere.[29] Data were collected at a sample-to-detector distance of 260 mm (calibrated using NIST SRM660b lanthanum hexaboride), and a 2θ range of 2°−48.5° was used in the Rietveld analysis. Samples of Cu-SSZ-13 were packed between plugs of quartz wool in 0.5 mm quartz capillaries and mounted in a Norby-type flow cell.[30] The samples were activated at a temperature of 773 K (heated using a hot air blower) under a flow of 50% oxygen in helium (10 mL/min), then cooled to room temperature, and exposed for 10 min to a flow of either NH_3 (5% in helium) or NO (4% in helium) after purging with pure helium (10 mL/min). Data were collected throughout the process with a data collection time of 10 s per frame and converted to 1-D powder patters using Fit2D[31,32] and the SNBL scaling software.[33]

Rietveld and difference Fourier analysis was carried out with the program TOPAS.[34] The initial model for the framework was taken from our earlier structure of Cu-SSZ-13 under SCR conditions.[8] After refinement of the framework model to obtain reasonable lattice parameters, background (12/9 term Chebshev polynomial for Cu-SSZ-13-NO/NH_3, respectively, plus a broad peak with refined Lorentzian crystallite size, position, and intensity parameters to fit the amorphous capillary scattering) scale and peak broadening values (the peak shape from BM01A is sufficiently symmetric that the TOPAS fundamental parameters size and strain macros can be used directly—in this case the Gaussian size and strain macros were applied) difference Fourier maps were used to locate the Cu and gas atoms. The scaling factor was obtained using the high angle data (which are not significantly affected by adsorption of molecules in a zeolite framework[35]) and fixed for determination of the difference maps using the whole powder pattern. The Cu atom was initially located in the *8r* window (in agreement with the structure determined by Andersen et al. using maximum entropy methods[11]), and further cycles of difference Fourier mapping revealed possible positions for the atoms of the adsorbed gases. In the final Rietveld refinements all framework atom positions were refined without restraints along with isotropic thermal parameters for the silicon and oxygen atoms (one parameter for each type), background, peak broadening, scale factor, lattice parameters, zero point correction, and occupancies for the non-framework atoms (a total of 34 refined parameters for the NO structure and 33 for the NH_3 structure).

2.3. Computational Details. Theoretical calculations are ideally suited to explore the geometries of the Cu coordinated complexes and their detailed molecular interactions.[36] Advances in both theoretical methodologies and applied model systems ensure that simulations are more realistic and able to capture relevant effects. Importantly, long-range van der Waals interactions which are known to be crucial for describing adsorption of guest molecules in zeolite systems can be included using the empirical corrections as developed by Grimme and co-workers (i.e., the DFT-D method).[37] Second, the nanoporous environment can be accounted for by using extended clusters[22] or periodic unit cells.[15,20,38−40] Although the investigated molecules NO and NH_3 are relatively small, the zeolite environment must be included to provide a realistic description of the coordinated complexes and their direct environment. In the present contribution, periodic DFT-D-based simulations are performed using large unit cells of Cu-SSZ-13. Such a periodic approach has the advantage over cluster models since it includes the full environment and no fictitious boundaries are introduced.

Density functional theory (DFT) geometry optimizations were carried out using the Gaussian plane wave (GPW) method as implemented in the CP2K software program.[41−44] The PBE exchange-correlation functional with additional pairwise dispersion corrections according to the D3 scheme of Grimme in combination with a double-ζ MOLOPT basis set with plane wave cutoff of 300 Ry was used.[37,45−48] The PBE functional was previously shown to provide accurate structures for Cu-SSZ-13 zeolites.[14,15,38,39]

The unit cell parameters were taken from crystallographic data of pure silica SSZ-13 and kept fixed during the geometry optimization. The employed Cu-exchanged unit cell contains 109 atoms, including 36 T-sites with corresponding oxygen atoms and one Cu^{2+} ion. To compensate for the charge on the Cu^{2+} ion, two silicon atoms were substituted by aluminum.[14] The double Si to Al substitution was done at the same locations of our previous investigation.[20] This leads to a Si/Al ratio of 17, which is close to the experimental value of 15 used in this study. This choice is possible since the applied unit cell corresponds with the hexagonal structure containing 36 T-sites. As a matter of comparison, previous studies by Göltl et al. apply the rhombohedral unit cell for the CHA topology, containing 12 T-sites.[14,15,38,39] These minimal unit cell calculations do not allow exploring structures with Al substitutions located in different *d6r* units, as is the case in our calculations. Moreover, a larger unit cell reduces the interaction of the copper complexes with their periodic images.

Atomic charges were calculated using the Hirshfeld-I (HI) partitioning scheme.[49] Several assessment studies have shown that the HI scheme leads to accurate electrostatic potentials[50,51] and that the HI charges are to some extent transferable, e.g., with respect to the choice of basis set[52] and conformational changes.[53] The charge distribution of the original Cu-containing SSZ-13 models as well as NO and NH_3 coordinated complexes were investigated. The performed HI analysis involves the PBE-D3 method and basis set specifications as used for the geometry optimizations. As any other partitioning scheme, it does not allow to directly determine the discrete oxidation numbers. We therefore focus on the observable

DOI: 10.1021/acs.jpcc.5b06875
J. Phys. Chem. C 2015, 119, 24393−24403

trends in atomic charges in order to describe the electron donation/accepting behavior. The partitioning was done by the in-house code Horton.[54]

In addition to static optimizations, *ab initio* molecular dynamics (MD) simulations are performed to include the effect of temperature and to assess the mobility of the Cu ions and the guest molecules. MD simulations have previously been applied in the frame of NH_3-SCR chemistry using Cu-SSZ-13 to derive IR spectra of the catalyst materials or NH_3 adsorption complexes.[20] MD simulations were performed on all atoms using the canonical ensemble at room temperature (300 K). After 3 ps through velocity rescaling,[55] the Nosé−Hoover thermostat[56] was used for 10 ps with a time step of 1 fs. Geometrical information was derived from the MD simulations; all post-processing was done using the program MD-tracks.[57]

3. RESULTS AND DISCUSSION

Initially we discuss the results obtained from the XRD data since this allowed us to properly identify the position of the Cu ions and subsequent complexes within the microporous volume. Thereafter, we discuss plausible complexes as determined from simulation before using both types of data to interpret the XANES and EXAFS results.

3.1. Exposure of NO to Cu-SSZ-13. *3.1.1. Synchrotron-Based in Situ Powder Diffraction (PD).* Figure 2 shows the observed, calculated, and difference patterns obtained from the Rietveld refinement of synchrotron PD data collected on Cu-SSZ-13 at room temperature after exposure to NO. The position of NO in the structure was determined as described in section 2.2.2. The difference Fourier map after determination of the Cu position is given in Figure S1 while the experimental parameters and goodness-of-fit factors are presented in Table S1 with the coordinates and selected bond lengths and angles obtained from the analysis shown in Tables S2 and S3, respectively. The average T−O (Si1−O) bond length (1.613 ± 0.004 Å) is slightly higher than the mean value of (1.594 ± 0.027 Å) as reported in a comparison of various pure silica zeolites.[58] Importantly, the Cu^{2+} ion was seen to locate in the center of the *8r* (see Figure 3). The Cu1−O distances are 3.440 Å (O2), 3.167 Å (O3), and 3.215 Å (O4); this is probably due to an averaging of the electron density from the Cu atom on the special position at (1/2, 1/2, 0) and is essentially in agreement with the more detailed maximum entropy study carried out by Andersen et al.,[11] in that the Cu is situated in the *8r*. Attempts to use the Cu position suggested by Andersen et al. resulted in a worse final *R* factor when refined against the diffraction data shown above.

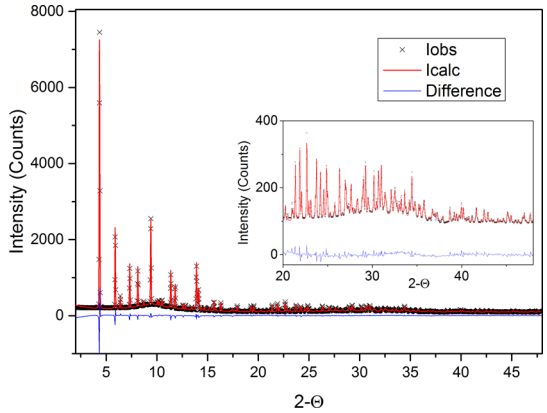

Figure 2. Observed, calculated, and difference patterns with the corresponding expected reflection positions obtained from the Rietveld refinement of powder diffraction data collected on Cu-SSZ-13 after exposure to NO at room temperature (labeled Cu-SSZ-13-NO) using a fixed zero error of 0.002. The inset illustrates the fit at high angle. Tables S1−S3 contain details of the information extracted from the Rietveld refinement.

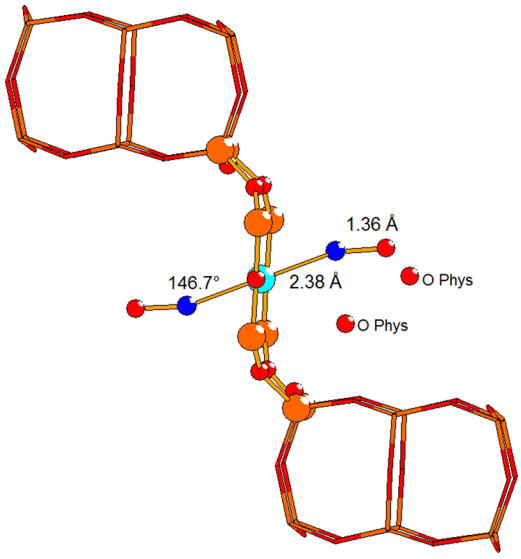

Figure 3. Model derived using difference Fourier maps from the diffraction data of Cu-SSZ-13-NO shown in Figure 2. Silicon atoms = orange, oxygen = red, Cu = pale blue, and N = dark blue. Key bond lengths and angles are labeled along with atoms assigned to the positions of possible physisorbed gas molecules in the *cha* cage. Note the appearance of two Cu−N−O interactions is due to symmetry and not indicative of two Cu−nitrosyl species. The asymmetric unit and additional structure views (including the presence of the second N component) are given in Figure S1.

Further electron density peaks were observed around the Cu and in the center of the *cha* cage. The components closest to the Cu were assigned as nitrogen atoms on the basis of recent work, since the similar X-ray scattering factors of O and N make them almost impossible to distinguish using X-rays.[8,11] The N atom (Cu1−N2 = 2.38 Å) has a neighboring Fourier peak at a distance of 1.36 Å, assigned as an oxygen atom (O5). The obtained Cu1−N2−O5 bond angle of 146.6° is remarkably the same as has recently been reported for a Cu−N−O (Cu−nitrosyl) complex in SSZ-13.[16] Two further oxygen atoms were added to the model on the Fourier peaks in the center of the *cha* cage (O_{phys}); these probably represent the location of NO which is physisorbed in the framework rather than bound to the Cu. Note that the approach used here allows determining of not only species coordinated to Cu but also physisorbed species, which cannot be accounted by the other techniques employed in this work. Additionally, we note an additional N at 2.16 Å away from the Cu (Cu1−N1; for clarity this is not shown here in Figure 3 but can be seen in Figure S1). This is close to a special position and has no neighboring peaks in the difference Fourier maps. This peak is almost certainly a manifestation of the disordered location of the NO molecules (due to dynamic disorder of the gas, averaging of NO locations in different parts of the crystal lattice and symmetry). The structure of the proposed model is shown in Figure 3. This model is clearly no more than an approximation of the true structure, averaged by disorder and symmetry; however, the

DOI: 10.1021/acs.jpcc.5b06875
J. Phys. Chem. C 2015, 119, 24393−24403

Rietveld fit is of good quality (*Rwp* = 3.386). Details of the refinement (including structural phase information, refined atomic positions, occupancies, symmetry, and thermal parameters) are summarized in Tables S1–S3.

The apparent bent nature of the NO–Cu^{2+} complex in combination with an NO bond distance of 1.36 Å could suggest that reduction of the Cu occurs during the formation of the NO–Cu complex.[59,60] Note that shifting the Cu away from the center of the *8r* would increase the Cu–N–O angle still further.

3.1.2. DFT Geometry Optimizations and MD Simulations. Based on the diffraction results, adsorption of NO at a Cu^{2+} site near the *8r* is modeled using periodic PBE-D3 simulations. Figure 4a depicts the detailed optimized geometries of the NO adsorbed complex, and Table 1 summarizes the resulting geometrical parameters.

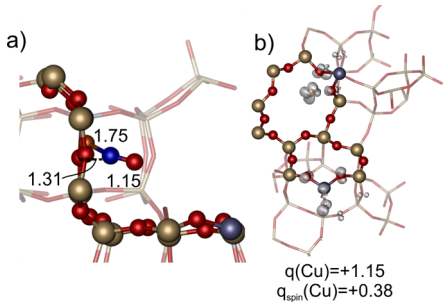

Figure 4. (a) Detailed view of optimized Cu–NO nitrosyl complex formed in SSZ-13 using static periodic PBE-D3 simulations, with Cu initially in the *8r*. Bond lengths are given in Å. The distance between the N of NO and the *8r* window is also indicated. (b) Isosurface of the spin density (gray lobes) of the Cu-SSZ-13 and computed HI (spin) charges using PBE-D3.

The copper ion remains approximately in the *8r* window upon NO adsorption with a theoretically obtained bond angle equal to ∼151° (Table 1), which is in very good agreement with the XRD data. The bond distances are of course shorter than those reported from the Rietveld analysis but provided the local structure model in order to perform a detailed multiple shell fit to the EXAFS data. The copper ion coordinates with two oxygen framework atoms, and in combination with the NO adsorption, the 3-fold coordination is maintained compared to the situation of the original Cu-SSZ-13 material.

The effect of temperature on the adsorption complexes is assessed by performing MD simulations at room temperature. Averaged geometrical parameters and computed variations σ are included in Table 1. The results clearly indicate that the averaged MD properties are in close agreement with those from the static geometry optimization obtained at 0 K. The variation of the copper ion location—relative to the averaged MD position—is indicative of the mobility of the Cu center (see Figures S3 and S4). The copper ions move around in a range of approximately 1 Å, in both a vertical and horizontal direction. The 10 ps MD simulations point out that the difference in mobility between the bare copper ions and those after adsorption of a NO molecule is very small at the investigated temperature of 300 K. It should be mentioned at this stage that in order to describe the Cu mobility in terms of a $deNO_x$ mechanism, the simulation lengths are too short, and more advanced methods, in particular accelerated MD techniques, provide an interesting approach.[61] Indeed, it has been shown

Table 1. Relevant Bond Distances [in Å] and Angles [in deg] of Adsorbed Complexes[a]

	theoretical values	
atom pair	static	dynamic
	Cu-SSZ-13-NO	
N–O	1.15	1.18 (0.08)
Cu–N	1.75	1.75 (0.05)
O–N–Cu	151	151 (12.6)
Cu–O	1.92	1.94 (0.05)
	2.02	1.98 (0.06)
Cu–T	2.75	2.74 (0.06)
	3.24	
	3.32	
	$[Cu(NH_3)_4]^{2+}$ complex -- Cu-SSZ-13-NH_3	
Cu–N	2.05	2.07 (0.07)
$Cu–O_{(framework)}$	2.57	3.10 (0.16)
	3.41	3.28 (0.19)
	3.44	3.06 (0.16)
	3.46	3.43 (0.12)
		av_min:[b] 2.94
Cu–T	3.47	3.95 (0.15)
	3.56	3.91 (0.14)
	4.10	4.24 (0.14)
	4.24	4.24 (0.17)
	3.78	3.78 (0.14)

[a]The static data result from geometry optimizations. The MD data are averaged parameters obtained from analyzing the 10 ps MD runs at room temperature. Standard variations σ of the MD data are also listed in parentheses. Note: T is a general label given to framework atoms which could be either Si^{4+} or Al^{3+}. [b]Due to the flexible nature of the $[Cu(NH_3)_4]^{2+}$ complex, hydrogen bonds between the hydrogens of the NH_3 molecules and the framework oxygen atoms are instantly formed and broken. Therefore, in addition to these averaged values, the "av_min" value is also reported, providing the average of the minimal Cu–O distance during the MD simulation.

that the Cu occupancy in the *6r* increases with increasing temperature either during calcination[6] or under standard SCR conditions.[8]

Next, the electronic charge density is partitioned over the multiple atoms in the system—according to the Hirshfeld-I (HI) scheme—resulting in indicative atomic HI charges to assess the possible reduction of the Cu^{2+} upon NO adsorption. Figure 4b displays the spin densities of the original Cu-SSZ-13 material, with indication of computed HI (spin) charges on the Cu center. There is also a non-negligible amount of spin density at the O atoms neighboring the Al positions. Upon NO adsorption, the charge on the Cu is found to be slightly increased (from 1.15 to 1.25) using the PBE-D3 functional. However, the charge is found to be slightly reduced (going from 1.50 to 1.40) when employing a hybrid B3LYP functional (in correspondence with previous results of Goeltl et al.[39]), involving the transfer of electrons to the framework.

3.1.3. Synchrotron-Based in Situ X-ray Absorption Near-Edge Structure (XANES). Figure 5 illustrates the Cu K-edge XANES spectra of Cu-SSZ-13 collected during calcination at 773 K and at RT after exposure to NO. The XANES spectra contain a weak pre-edge feature at ∼8977 eV (magnified inset (b)), attributable to a dipole-forbidden/quadrupole allowed 1s to 3d transition observed in Cu^{2+} systems.[1,8] Although there are not many observations made to define this pre-edge peak, it is clear that the intensity is slightly greater in the Cu-SSZ-13 sample recorded at 773 K than for the Cu-SSZ-13-NO sample.

DOI: 10.1021/acs.jpcc.5b06875
J. Phys. Chem. C 2015, 119, 24393–24403

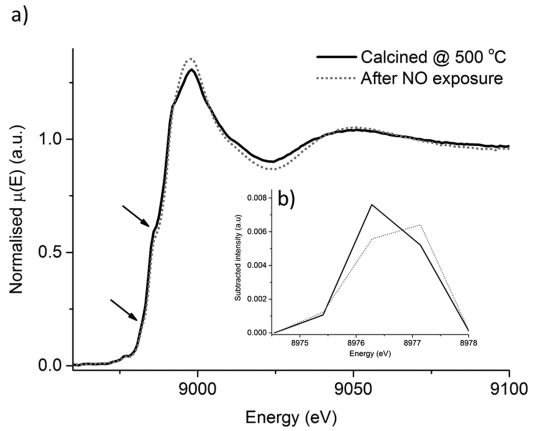

Figure 5. (a) Cu K-edge XANES spectra of Cu-SSZ-13 during calcination in 5% O_2/He at 773 K and after exposure to NO (collected at room temperature). (b) Magnification of the background subtracted pre-edge feature (1) at ∼8977 eV.

A second following pre-edge feature (first arrow) is seen at ∼8982 eV and has previously been assigned to a transition from a 1s to the doubly degenerate $4p_{xy}$ orbitals in Cu^+ systems.[1,8,62,63] The absorption threshold (second arrow at ∼8986 eV) is an often observed feature in copper-containing zeolite systems and is attributed to a Cu^{2+} 1s to $4p_z$ + ligand−Cu^{2+} charge-transfer excitation, first identified from studies on the planar $Cu(OH)_2$ system.[1,8,64] The given pre-edge features and position of the rising absorption edge suggest that the Cu environment is broadly similar in both samples and that the local environment around the Cu species does not appear to change very much after NO exposure. However, the small reduction observed in the pre-edge peak as well as the appearance of a feature at 8982 eV suggests that perhaps a partial reduction of all Cu^{2+} to $Cu^{<2+}$ or a total reduction of some of the copper species to Cu^+ occurs as a result of the interaction between Cu and NO. We note, however, that it is not possible to rule out a change in coordination environment of the Cu^{2+} to a state with higher symmetry might also be a cause of the reduction in the pre-edge peak intensity. Indeed, this would be in agreement with previous works showing that NO exposure alone does not lead to a significant Cu reduction.[18,19]

3.1.4. Synchrotron-Based in Situ Extended X-ray Absorption Fine Structure (EXAFS). Analysis of the k^3-weighted EXAFS data was performed considering only single scattering paths. The results of the analysis (fit to the data) in both *k*- and *r*-space (Fourier transformed (FT) data) are given in Figure 6. The initial models were based on the information obtained from the computer simulations shown in Table 1 and further optimized to account for any local (real-space) differences in the Cu environment. The obtained near-neighbor distances, coordination numbers, and Debye−Waller factors are listed in Table 2.

Table 2. Parameters Obtained from Analysis of Cu K-Edge k^3-Weighted EXAFS Data (Based on the Energy-Minimized Static Model Detailed in Table 1); Cu-SSZ-13 Collected at Room Temperature after Exposure to NO[a]

shells	*r* (Å)	*N*	$2\sigma^2$ (Å^2)
Cu−O	1.95	2	0.008
Cu−N	1.80	1	0.008
Cu−T1	2.76	1	0.027
Cu−T2	3.16	2	0.031
	R = 21.13; E_f = 0 eV		

[a] *r* = averaged distance over 1 shell; *N* = coordination number; σ = Debye−Waller factor; *R* = statistical goodness of fit factor; E_f = Fermi energy (edge position).

The EXAFS data for which models were taken from the simulation for Cu in the *8r* fit well to the proposal of ∼3 short Cu−O contributions at ∼1.95 Å in addition to a shorter Cu−N interaction at ∼1.80 Å—much shorter than the distances reported from an analysis of the diffraction data which are symmetry averaged, but entirely consistent with previous analyses of Cu in SSZ-13 and other zeolites.[1] We note that the Debye−Waller factor obtained is very reasonable for a single Cu−N(O) contribution as opposed to >1. The short Cu−N distance observed is thought to originate from the NO acting as a π-acceptor ligand, typical in both linear and bent Me−NO complexes.[60] To complete the model, additional Cu−T distances from the SSZ-13 framework at 2.76 and 3.16 Å are also found.

3.2. Interaction with NH_3. The same procedure as with NO was used to study the interaction of NH_3 with Cu in Cu-SSZ-13.

3.2.1. Synchrotron-Based in Situ PD. Figure 7 shows the observed, calculated, and difference patterns obtained from the Rietveld refinement of synchrotron PD data collected on Cu-

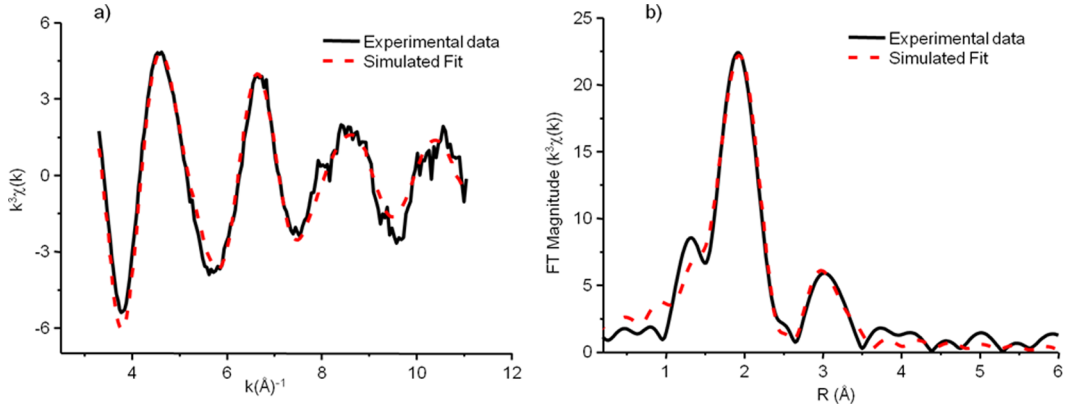

Figure 6. (a) Isolated Cu K-edge k^3-weighted EXAFS experimental (black solid line) and fitted (red dashed line) *k*-plot and associated Fourier transform and (b) of the EXAFS data collected on Cu-SSZ-13 at room temperature after exposure to NO at room temperature.

DOI: 10.1021/acs.jpcc.5b06875
J. Phys. Chem. C 2015, 119, 24393−24403

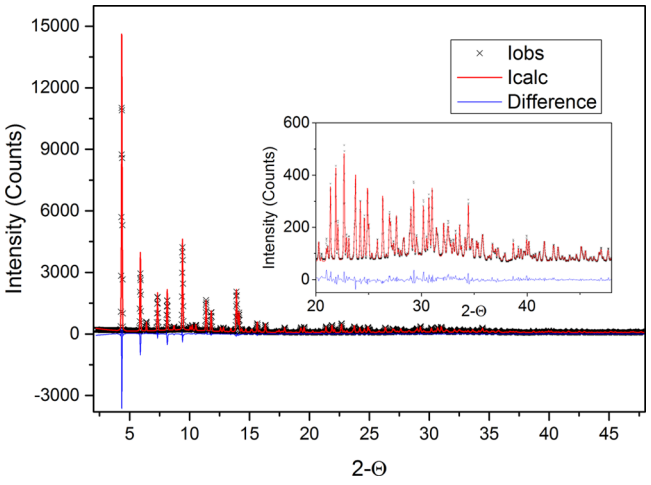

Figure 7. Observed, calculated, and difference patterns with the corresponding expected reflection positions obtained from the Rietveld refinement of powder diffraction data collected on Cu-SSZ-13 after exposure to NH_3 at room temperature (labeled Cu-SSZ-13-NH_3). The inset illustrates the fit at high angle. Tables S5−S7 contain details of the information extracted from the Rietveld refinement.

SSZ-13 at room temperature after exposure to NH_3. Tables S5−S7 list the corresponding goodness-of-fit values, atomic coordinates, and bond distances and angles of interest, respectively.

Cu is again located in the *8r* window as shown in Figure 8. Further difference maps after location of the Cu revealed peaks

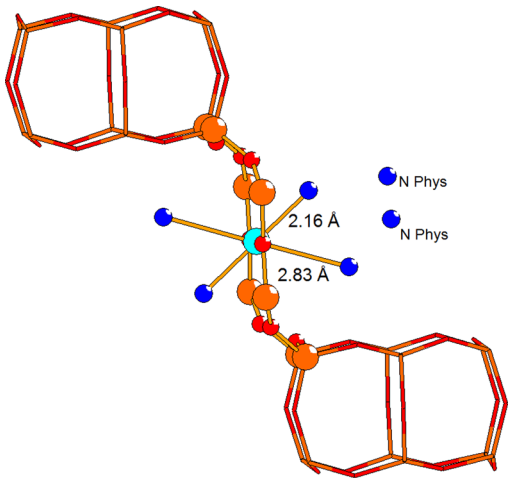

Figure 8. Model derived using difference Fourier maps from the diffraction data of Cu-SSZ-13 shown in Figure 7. Cu−N bond lengths are labeled along with atoms assigned to positions in the *cha* cage probably occupied by physisorbed nitrogen. Silicon atoms = orange, oxygen = red, Cu = pale blue, and N = dark blue. The asymmetric unit and further views are shown in Figure S5.

at distances of 2.16 Å (N3) and 2.83 Å (N4) from the Cu; these were assigned as coordinated nitrogen. Two further peaks in the center of the *cha* cage are assigned to physisorbed ammonia (N1, N2). The crystal structure model is shown in Figure 8.

The crystal structure model is as for Cu-SSZ-13-NO, not a truly accurate picture of the disordered structure of adsorbed ammonia in Cu-SSZ-13, but gives a good indication as to the location of the chemisorbed gas and the geometry of the Cu-SSZ-13-NH_3 complex. The final *Rwp* for the refinement was 4.878. Full details of the refinement atomic positions and bond lengths and angles are given in Tables S5−S7.

3.2.2. DFT Geometry Optimizations and MD Simulations. Adsorption of ammonia on copper in its initial configuration located in the *8r* window was modeled with increasing the number of adsorbed ammonia molecules. The resulting structures can be found in Figure S8. Addition of two ammonia molecules did not result in a linear N−Cu−N complex as seen by Giordanino et al.;[22] the obtained angle from the geometry optimization equals 99°. During these simulations it was observed that the copper ion remained rather localized, i.e., present near the *8r* window. Because of steric constraints of these windows (which are only 3.8 Å wide), addition of a fourth ammonia molecule was highly unfavorable. In particular, during optimization the fourth ammonia molecule drifts toward the *cha* cage, suggesting a 3-fold coordinated structure when the copper is in the *8r*. A $[Cu(NH_3)_4]^{2+}$ structure with the central Cu located in the *8r* window could nevertheless be obtained (Figure 9b), although this 4-fold coordinated structure is 97 kJ/

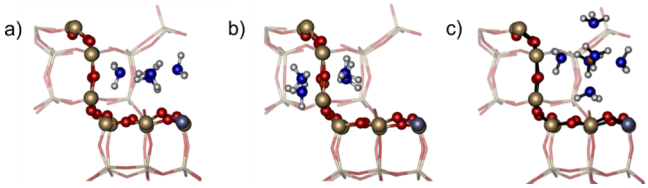

Figure 9. Optimized $[Cu(NH_3)_4]^{2+}$ complexes using static PBE-D3 simulations, with the copper ion originally located in (a) the CHA cage and (b) the middle of the *8r*. (c) Optimized $[Cu(NH_3)_6]^{2+}$ complex using static PBE-D3 simulations, with the Cu^{2+} ion originally located in the *cha* cage.

mol less stable compared to the 3-fold coordinated structure with the additional ammonia molecule in the *cha* pore. Important geometrical distances are included in Table 1. This complex was however 147 kJ/mol higher in energy (at 0 K) than the copper−amine complex present in the center of the pore as has been previously reported by some of us (Figure 9a).[20] Once formed, the $[Cu(NH_3)_4]^{2+}$ with the copper in the *8r* remains metastable, as observed during the 10 ps MD run. Averaged MD simulations indicate a minor influence of temperature on the relevant bond lengths (see Table 1). The extent of Cu mobility at room temperature (see Figures S3 and S4) is similar to the aforementioned situations for NO adsorption. Overall, our simulations suggest a strong preference for the tetraamine complex $[Cu(NH_3)_4]^{2+}$ to reside in the cage rather than the *8r*.

In addition to the tetraamine complexes, also a hexaamine $[Cu(NH_3)_6]^{2+}$ complex was modeled. The optimized geometry (shown in Figure 9c) corresponds with a distorted octahedral structure which is located in the center of the pore. The Cu−N bond lengths in the *c*-axis (i.e., along the length of the *cha* cage) are 2.294 and 2.618 Å, whereas the distance between the copper and the four other amine molecules is on average 2.093 Å. This $[Cu(NH_3)_6]^{2+}$ complex exhibits a high stability; i.e., the adsorption of the two additional ammonia molecules corresponds to an adsorption energy (at 0 K) of 378 kJ/mol, indicating that the formation of an hexaamine complex residing in the center of the large pore is energetically very favorable. It is important to stress, however, that a multitude of hexaamine complexes, differing in precise bond lengths and hence

DOI: 10.1021/acs.jpcc.5b06875
J. Phys. Chem. C 2015, 119, 24393−24403

distortion from the octahedral symmetry, could also be expected.

3.2.3. Synchrotron-Based in Situ XANES. Figure 10 illustrates the Cu K-edge XANES spectra of Cu-SSZ-13 collected during calcination at 773 K and at RT after exposure to NH_3. Both XANES spectra again contain a weak pre-edge feature at ~8977 eV (magnified inset (b)), typical for Cu^{2+} systems as discussed in section 3.1.3; however, this feature is much weaker in the NH_3 exposed sample when compared to the calcined sample. The resulting drop in intensity therefore could be either attributed to a reduction to Cu^+ or else to a change in coordination geometry around Cu^{2+} to a higher symmetry (either to O_h or D_{4h} both point groups possessing inversion symmetry rendering the 1s−3d dipole transition disallowed). We note however the absence of a Cu^+ charge transfer band at 8992 eV (lower solid black arrow) which was observed in the NO exposed sample. The double resonance at the top of the rising absorption edge (upper solid black arrow) was observed by some of us previously under standard SCR conditions during low NO_x conversion but also by others.[8,65,66] This distinct feature clearly observable in the spectrum has previously been assigned to Cu^{2+} in a square-planar arrangement, proposed by Chaboy et al. to occur as a result of two final configurations of $3d^9$ and $d^{10}L$ of the absorber atom (L = ligand hole).[67] Contrary to the case of NO, and upon comparison to the reference spectrum, the XANES in this case suggests an extensive Cu−NH_3 interaction, resulting in a change in the local environment for the absorbing Cu. Importantly, no significant change in Cu oxidation state is observed.

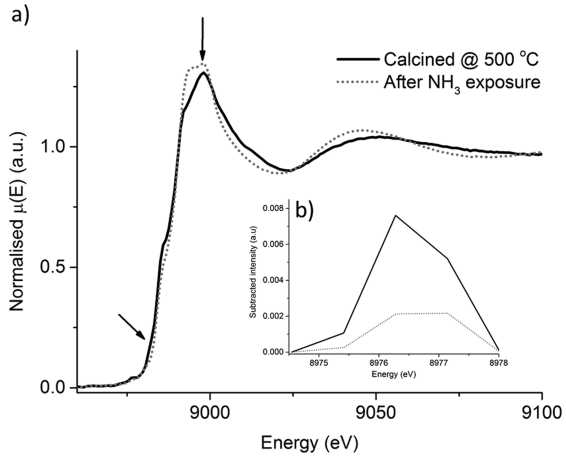

Figure 10. (a) Cu K-edge XANES spectra of Cu-SSZ-13 during calcination in 5% O_2/He at 773 K and after exposure to NH_3 (collected at room temperature). (b) Magnification of the background subtracted pre-edge feature (1) at ~8977 eV.

3.2.4. Synchrotron-Based in Situ EXAFS. The corresponding EXAFS data were again analyzed considering only single scattering paths. Figure 11 illustrates the experimental data and simulated fits of the k^3-weighted EXAFS data and the corresponding with the results of the analysis listed in Table 3. The first and major contribution in the phase-corrected EXAFS-FT observed at ~2.00 Å could be fit to the presence of ca. ~4 N atoms at a distance of 2.04 Å. The slightly larger Debye−Waller factors obtained for the first shell Cu−N contributions reflects a higher static disorder of the amine ligands in comparison to the oxygen ligands from the zeolite framework for either the calcined or NO exposed sample. The second clear contribution at ca. >2.50 Å in the EXAFS-FT (Figure 11b) corresponded to what we propose to be a second contribution at 2.71 Å with a coordination number of ≥1. The large Debye−Waller factor for this contribution in conjunction with a high degree of correlation with the coordination number renders it difficult to unambiguously assign an integer coordination number, and as a result, there is some debate as to whether it is possible for EXAFS to determine between Cu^{2+} ions in distorted 5- or 6-fold coordination.[27] Perhaps the third significant observation in the FT is a lack of a contribution around 3 Å ascribable to Cu^{2+}−$O/Si_{(framework)}$, suggesting a different Cu^{2+} cation location to that seen for the Cu−NO complex. Indeed, this complete lack of a signal in this part of the FT would be consistent with a Cu complex located in the

Table 3. Parameters Obtained from Analysis of Cu K-Edge k^3-Weighted EXAFS Data of Cu-SSZ-13 Collected at Room Temperature after Exposure to NH_3[a]

temperature	shells	r (Å)	N	$2\sigma^2$ (Å^2)
after exposure to NH_3	Cu−N	2.04	4.0	0.016
	Cu−N	2.71	1.2	0.021
		R = 22.39; E_f = −0.6793		

[a] r = averaged distance over 1 shell; N = coordination number; σ = Debye−Waller factor; R = statistical goodness of fit factor; E_f = Fermi energy (edge position).

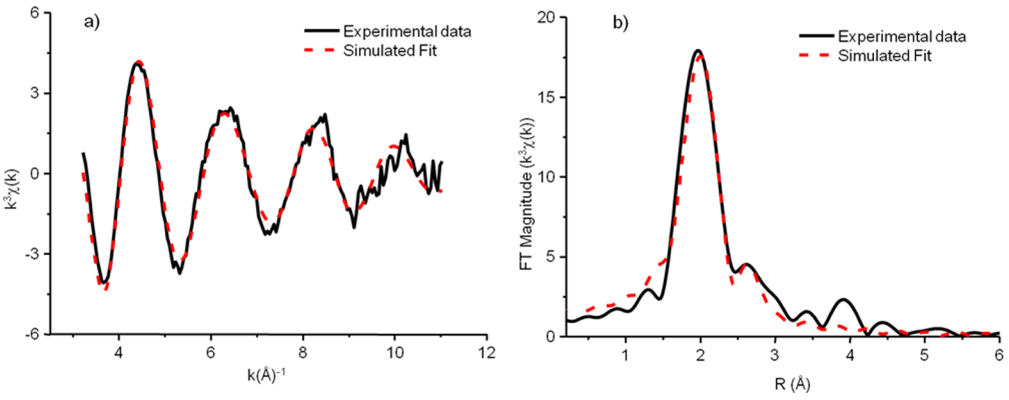

Figure 11. Isolated Cu K-edge k^3-weighted EXAFS experimental (black solid line) and fitted (red dashed line) k-plot (a) and associated Fourier transform (b) of the EXAFS data collected on Cu-SSZ-13 at room temperature after exposure to NH_3 at room temperature.

DOI: 10.1021/acs.jpcc.5b06875
J. Phys. Chem. C 2015, 119, 24393−24403

zeolite cages as suggested by the simulations rather than the *8r* as indicated by the PD data.

4. SUMMARY AND CONCLUSIONS

The interaction of NO and NH_3 with Cu ions in Cu-SSZ-13 was studied using combined XAFS/PD after exposure at room temperature, with the resultant model geometries optimized with DFT. In the NO-exposed sample Cu cations were seen to occupy the *8r* site; no discernible presence of Cu in the *6r* could be detected. In contrast, in the NH_3-exposed sample whilst PD suggests a similar tendency for Cu to occupy the *8r*, computational simulations suggest a preference for Cu amine complexes to locate in the cages of the CHA structure while XANES and EXAFS indicate the coordination must be 6-fold and is Jahn−Teller distorted. We elaborate further below.

For the NO-exposed sample, the Cu^{2+} cation forms a complex comprising two Cu−O bonds (to the SSZ-13 framework) and a third Cu−N−O interaction in which the Cu−nitrosyl bond angle is ∼150°, rendering it an "intermediate" nitrosyl complex.[60] Importantly, these results are in complete agreement with those previously reported by Kwak et al., wherein a Cu−nitrosyl complex was proposed to be a key intermediate in the NH_3-SCR reaction of NO on Cu-SSZ-13.[16]

The short Cu−N distance determined from DFT (and fitted in the EXAFS) as well as small change in the Cu XANES suggests that the Cu−NO interaction is a "Cu^+-like" although the remaining Cu−O "anchor points" to the *8r* maintain Cu in a predominantly 2+ oxidation state. Further support for this proposition comes from previous observations showing that Cu in the *8r* is more reducible than Cu in the *6r* (and more reducible than Cu oxides); it seems unlikely that the observed reduction is due to some unseen (diffraction silent) Cu species. As a result of the partial reduction of Cu via the formation of the Cu−nitrosyl complex, the NO molecule becomes partially oxidized and the N═O bond distance is slightly longer, ∼1.18 Å (although from PD this distances appears much longer due to symmetry averaging), than for gas-phase NO.[59] These results are in excellent agreement with data previously reported by Pulido and Nachtigall for mononitrosyl Cu−N−O complexes in ferrierite although in this study the Cu cation possesses a charge of +1.[68]

Conversely, NH_3 appears to have an extensive interaction with Cu^{2+} forming a Cu^{2+} containing complex which is likely 6-coordinate, i.e., $[Cu(NH_3)_6]^{2+}$. This we rationalize based on a preference for the Cu−amine complex to locate in the cages of the structure and evidence for axial NH_3 contributions at 2.71 Å in the EXAFS data (in addition to four shorter equatorial contributions at ∼2.04 Å). We rule out the possibility of 5-fold coordination on the basis of the presence of long axial contributions and a weak pre-edge peak which, in the absence of evidence for Cu reduction, suggests a local environment possessing inversion symmetry (i.e., O_h as opposed to C_{4v} or D_{3h}). The lack of a definitive coordination number for the axial contribution (i.e., whether 1 or 2 ligands are present) reflects the difficulty in EXAFS analysis to extract reliable coordination numbers from contributions which are long and probably dynamic as well as of likely differing lengths.[60] The inability of PD to distinguish between Cu located in the *8r* from that of Cu in the cage can be understood in terms of the smearing of the electron density across the two sites, and in the difficulty in being able to resolve this, especially at the loadings present in our samples. However, these results suggest that the Cu in Cu-SSZ-13 can contribute significantly to the NH_3 storage capacity (which can be useful when operating under NO-rich conditions); it is also likely to be highly mobile.

The combination of two techniques, one based on directly obtaining information from real space (XAFS) and another based on deriving information by exploiting the reciprocal space (PD), is crucial to obtaining detailed structural models. The obvious drawback of using X-ray techniques lies in the fact that they cannot distinguish between elements with closely related absorption and scattering coefficients such as N and O, which can limit the type of conclusions that can be made. However, even with such information it is also necessary to verify and refine these models with the use of computational methodologies to obtain the reliable structures necessary to determine all important structure−function relationships in catalytic materials. We note that although the data reported here are obtained under conditions that are far from those in which this catalytic system is typically employed, they do provide a useful starting point toward understanding the formation and role that such complexes play in phenomena such as adsorption, storage, and catalytic reaction, which are key processes that enable these catalytic systems to carry out their intended function.

■ ASSOCIATED CONTENT

Supporting Information

The Supporting Information is available free of charge on the ACS Publications website at DOI: 10.1021/acs.jpcc.5b06875.

PD analysis (Rietveld refinement; atomic coordinates, thermal parameters and site occupancies; bond lengths and angles; difference Fourier maps and asymmetric units) and computational results (study of the variation of Cu ion location; study of Cu−ammonia complexes as a function of increasing ammonia molecules) (PDF)

■ AUTHOR INFORMATION

Corresponding Author

*E-mail: andrew.beale@ucl.ac.uk (A.M.B.).

Notes

The authors declare no competing financial interest.

■ ACKNOWLEDGMENTS

EPSRC is thanked for funding support to Andrew M. Beale and I. Lezcano-Gonzalez. The authors thank Sachem Inc. for kindly providing the template (ZeoGen 2825) used in the synthesis of SSZ-13. ESRF is thanked for access to perform both XAFS and PD measurements. Herman Emerich and Dmitri Chernyshov (beamline scientists, SNBL) are thanked for their contributions toward enabling the measurements to be performed. This work was also supported by the Fund for Scientific Research Flanders (FWO), the Research Board of Ghent University (BOF), and BELSPO in the frame of IAP P7/05. The computational resources and services used in this work were provided by the VSC (Flemish Supercomputer Center), funded by the Hercules Foundation and the Flemish Government - department EWI. Ir. Tom Van den Heede is also acknowledged for performing simulations on the NO adsorption.

■ REFERENCES

(1) Beale, A. M.; Gao, F.; Lezcano-Gonzalez, I.; Peden, C. H. F.; Szanyi, J. Recent Advances in Automotive Catalysis for NOx Emission Control by Small-Pore Microporous Materials. *Chem. Soc. Rev.* **2015**, *44*, 7371.

DOI: 10.1021/acs.jpcc.5b06875
J. Phys. Chem. C 2015, 119, 24393−24403

(2) Deka, U.; Lezcano-Gonzalez, I.; Weckhuysen, B. M.; Beale, A. M. Local Environment and Nature of Cu Active Sites in Zeolite-Based Catalysts for the Selective Catalytic Reduction of NOx. *ACS Catal.* **2013**, *3*, 413−427.
(3) Gao, F.; Kwak, J.; Szanyi, J.; Peden, C. F. Current Understanding of Cu-Exchanged Chabazite Molecular Sieves for Use as Commercial Diesel Engine DeNOx Catalysts. *Top. Catal.* **2013**, *56*, 1441−1459.
(4) Iwamoto, M.; Yahiro, H.; Tanda, K.; Mizuno, N.; Mine, Y.; Kagawa, S. Removal of Nitrogen Monoxide through a Novel Catalytic Process. 1. Decomposition on Excessively Copper-Ion-Exchanged ZSM-5 Zeolites. *J. Phys. Chem.* **1991**, *95*, 3727−3730.
(5) König, A.; Held, W.; Richter, T. Lean-Burn Catalysts from the Perspective of a Car Manufacturer. Early Work at Volkswagen Research. *Top. Catal.* **2004**, *28*, 99−103.
(6) Fickel, D. W.; Lobo, R. F. Copper Coordination in Cu-SSZ-13 and Cu-SSZ-16 Investigated by Variable-Temperature XRD. *J. Phys. Chem. C* **2010**, *114*, 1633−1640.
(7) Korhonen, S. T.; Fickel, D. W.; Lobo, R. F.; Weckhuysen, B. M.; Beale, A. M. Isolated Cu2+ Ions: Active Sites for Selective Catalytic Reduction of NO. *Chem. Commun.* **2011**, *47*, 800−802.
(8) Deka, U.; Juhin, A.; Eilertsen, E. A.; Emerich, H.; Green, M. A.; Korhonen, S. T.; Weckhuysen, B. M.; Beale, A. M. Confirmation of Isolated Cu2+ Ions in Ssz-13 Zeolite as Active Sites in NH3-Selective Catalytic Reduction. *J. Phys. Chem. C* **2012**, *116*, 4809−4818.
(9) Kwak, J. H.; Zhu, H.; Lee, J. H.; Peden, C. H. F.; Szanyi, J. Two Different Cationic Positions in Cu-SSZ-13? *Chem. Commun.* **2012**, *48*, 4758−4760.
(10) Gao, F.; Walter, E. D.; Karp, E. M.; Luo, J.; Tonkyn, R. G.; Kwak, J. H.; Szanyi, J.; Peden, C. H. F. Structure−Activity Relationships in NH3-SCR over Cu-SSZ-13 as Probed by Reaction Kinetics and EPR Studies. *J. Catal.* **2013**, *300*, 20−29.
(11) Andersen, C. W.; Bremholm, M.; Vennestrom, P. N. R.; Blichfeld, A. B.; Lundegaard, L. F.; Iversen, B. B. Location of Cu^{2+} in CHA Zeolite Investigated by X-Ray Diffraction Using the Rietveld/Maximum Entropy Method. *IUCrJ* **2014**, *1*, 382−386.
(12) Borfecchia, E.; Lomachenko, K. A.; Giordanino, F.; Falsig, H.; Beato, P.; Soldatov, A. V.; Bordiga, S.; Lamberti, C. Revisiting the Nature of Cu Sites in the Activated Cu-SSZ-13 Catalyst for SCR Reaction. *Chem. Sci.* **2015**, *6*, 548−563.
(13) Kwak, J. H.; Varga, T.; Peden, C. H. F.; Gao, F.; Hanson, J. C.; Szanyi, J. Following the Movement of Cu Ions in a SSZ-13 Zeolite During Dehydration, Reduction and Adsorption: A Combined In Situ TP-XRD XANES/DRIFTS Study. *J. Catal.* **2014**, *314*, 83−93.
(14) Göltl, F.; Bulo, R. E.; Hafner, J.; Sautet, P. What Makes Copper-Exchanged SSZ-13 Zeolite Efficient at Cleaning Car Exhaust Gases? *J. Phys. Chem. Lett.* **2013**, *4*, 2244−2249.
(15) Göltl, F.; Hafner, J. Structure and Properties of Metal-Exchanged Zeolites Studied Using Gradient-Corrected and Hybrid Functionals. I. Structure and Energetics. *J. Chem. Phys.* **2012**, *136*, 064501.
(16) Kwak, J. H.; Lee, J. H.; Burton, S. D.; Lipton, A. S.; Peden, C. H. F.; Szanyi, J. A Common Intermediate for N2 Formation in Enzymes and Zeolites: Side-on Cu−Nitrosyl Complexes. *Angew. Chem., Int. Ed.* **2013**, *52*, 9985−9989.
(17) Szanyi, J.; Kwak, J. H.; Zhu, H.; Peden, C. H. F. Characterization of Cu-SSZ-13 NH3 SCR Catalysts: An in Situ FTIR Study. *Phys. Chem. Chem. Phys.* **2013**, *15*, 2368−2380.
(18) Paolucci, C.; Verma, A. A.; Bates, S. A.; Kispersky, V. F.; Miller, J. T.; Gounder, R.; Delgass, W. N.; Ribeiro, F. H.; Schneider, W. F. Isolation of the Copper Redox Steps in the Standard Selective Catalytic Reduction on Cu-SSZ-13. *Angew. Chem., Int. Ed.* **2014**, *53*, 11828−11833.
(19) Janssens, T. V. W.; Falsig, H.; Lundergaard, L. F.; Vennestrøm, P. N. R.; Rasmussen, S. B.; Moses, P. G.; Giordanino, F.; Borfecchia, E.; Lomachenko, K. A.; Lamberti, C.; et al. A Consistent Reaction Scheme for the Selective Catalytic Reduction of Nitrogen Oxides with Ammonia. *ACS Catal.* **2015**, *5*, 2832−2845.
(20) Lezcano-Gonzalez, I.; Deka, U.; Arstad, B.; Van Yperen-De Deyne, A.; Hemelsoet, K.; Waroquier, M.; Van Speybroeck, V.; Weckhuysen, B. M.; Beale, A. M. Determining the Storage, Availability and Reactivity of NH3 within Cu-Chabazite-Based Ammonia Selective Catalytic Reduction Systems. *Phys. Chem. Chem. Phys.* **2014**, *16*, 1639−1650.
(21) Zhu, H.; Kwak, J. H.; Peden, C. H. F.; Szanyi, J. In Situ Drifts-MS Studies on the Oxidation of Adsorbed NH3 by NOx over a Cu-SSZ-13 Zeolite. *Catal. Today* **2013**, *205*, 16−23.
(22) Giordanino, F.; Borfecchia, E.; Lomachenko, K. A.; Lazzarini, A.; Agostini, G.; Gallo, E.; Soldatov, A. V.; Beato, P.; Bordiga, S.; Lamberti, C. Interaction of NH3 with Cu-SSZ-13 Catalyst: A Complementary FTIR, XANES, and XES Study. *J. Phys. Chem. Lett.* **2014**, *5*, 1552−1559.
(23) Moreno-González, M.; Hueso, B.; Boronat, M.; Blasco, T.; Corma, A. Ammonia-Containing Species Formed in Cu-Chabazite as per In Situ EPR, Solid-State NMR, and DFT Calculations. *J. Phys. Chem. Lett.* **2015**, *6*, 1011−1017.
(24) van Beek, W.; Safonova, O. V.; Wiker, G.; Emerich, H. SNBL, a Dedicated Beamline for Combined in Situ X-Ray Diffraction, X-Ray Absorption and Raman Scattering Experiments. *Phase Transitions* **2011**, *84*, 726−732.
(25) Newville, M. Ifeffit: Interactive XAFS Analysis and FEFF Fitting. *J. Synchrotron Radiat.* **2001**, *8*, 322−324.
(26) Ravel, B.; Newville, M. Athena, Artemis, Hephaestus: Data Analysis for X-Ray Absorption Spectroscopy Using Ifeffit. *J. Synchrotron Radiat.* **2005**, *12*, 537−541.
(27) Kervinen, K.; Bruijnincx, P. C. A.; Beale, A. M.; Mesu, J. G.; van Koten, G.; Klein Gebbink, R. J. M.; Weckhuysen, B. M. Zeolite Framework Stabilized Copper Complex Inspired by the 2-His-1-Carboxylate Facial Triad Motif Yielding Oxidation Catalysts. *J. Am. Chem. Soc.* **2006**, *128*, 3208−3217.
(28) Lytle, F. W.; Sayers, D. E.; Stern, E. A. Report of the International Workshop on Standards and Criteria in X-Ray Absorption-Spectroscopy - March 7−9, 1988 - Brookhaven-National-Laboratory. *Phys. B* **1989**, *158*, 701−722.
(29) http://www.esrf.eu/UsersAndScience/Experiments/CRG/BM01/bm01-a, access date: 16 September, 2015.
(30) Norby, P. In-Situ Time Resolved Synchrotron Powder Diffraction Studies of Syntheses and Chemical Reactions. *Mater. Sci. Forum* **1996**, *228−231*, 147−152.
(31) http://www.esrf.eu/computing/scientific/FIT2D/, access date: 16 September, 2015.
(32) Hammersley, A. P.; Svensson, S. O.; Hanfland, M.; Fitch, A. N.; Hausermann, D. Two-Dimensional Detector Software: From Real Detector to Idealised Image or Two-Theta Scan. *High Pressure Res.* **1996**, *14*, 235−248.
(33) Dyadkin, V. http://www.esrf.eu/home/UsersAndScience/Experiments/CRG/BM01/bm01-a/image.htm/snbl-tool-box.html, access date: 16 September, 2015.
(34) Coelho, A. A. TOPAS V4.1, Bruker AXS, 2006.
(35) McCusker, L. B.; Von Dreele, R. B.; Cox, D. E.; Louer, D.; Scardi, P. Rietveld Refinement Guidelines. *J. Appl. Crystallogr.* **1999**, *32*, 36−50.
(36) Van Speybroeck, V.; Hemelsoet, K.; Joos, L.; Waroquier, M.; Bell, R. G.; Catlow, C. R. A. Advances in Theory and Their Application within the Field of Zeolite Chemistry. *Chem. Soc. Rev.* **2015**, *44*, 7044.
(37) Grimme, S.; Antony, J.; Ehrlich, S.; Krieg, H. A Consistent and Accurate Ab Initio Parametrization of Density Functional Dispersion Correction (DFT-D) for the 94 Elements H-Pu. *J. Chem. Phys.* **2010**, *132*, 154104.
(38) Göltl, F.; Hafner, J. Structure and Properties of Metal-Exchanged Zeolites Studied Using Gradient-Corrected and Hybrid Functionals. II. Electronic Structure and Photoluminescence Spectra. *J. Chem. Phys.* **2012**, *136*, 064502.
(39) Göltl, F.; Hafner, J. Structure and Properties of Metal-Exchanged Zeolites Studied Using Gradient-Corrected and Hybrid Functionals. III. Energetics and Vibrational Spectroscopy of Adsorbates. *J. Chem. Phys.* **2012**, *136*, 064503.

DOI: 10.1021/acs.jpcc.5b06875
J. Phys. Chem. C 2015, 119, 24393−24403

(40) Van Speybroeck, V.; De Wispelaere, K.; Van der Mynsbrugge, J.; Vandichel, M.; Hemelsoet, K.; Waroquier, M. First Principle Chemical Kinetics in Zeolites: The Methanol-to-Olefin Process as a Case Study. *Chem. Soc. Rev.* **2014**, *43*, 7326−7357.
(41) VandeVondele, J.; Krack, M.; Mohamed, F.; Parrinello, M.; Chassaing, T.; Hutter, J. Quickstep: Fast and Accurate Density Functional Calculations Using a Mixed Gaussian and Plane Waves Approach. *Comput. Phys. Commun.* **2005**, *167*, 103−128.
(42) Lippert, B. G.; Parrinello, J. H.; Michele, A. Hybrid Gaussian and Plane Wave Density Functional Scheme. *Mol. Phys.* **1997**, *92*, 477−488.
(43) Lippert, G.; Hutter, J.; Parrinello, M. The Gaussian and Augmented-Plane-Wave Density Functional Method for Ab Initio Molecular Dynamics Simulations. *Theor. Chem. Acc.* **1999**, *103*, 124−140.
(44) Hutter, J.; Iannuzzi, M.; Schiffmann, F.; VandeVondele, J. Cp2k:Atomistic Simulations of Condensed Matter Systems. *Wiley Interdisciplinary Reviews. Computational Molecular Science* **2014**, *4*, 15−25.
(45) Perdew, J.; Burke, K.; Ernzerhof, M. Generalized Gradient Approximation Made Simple. *Phys. Rev. Lett.* **1996**, *77*, 3865−3868.
(46) Perdew, J.; Ruzsinszky, A.; Csonka, G.; Vydrov, O.; Scuseria, G.; Constantin, L.; Zhou, X.; Burke, K. Restoring the Density-Gradient Expansion for Exchange in Solids and Surfaces. *Phys. Rev. Lett.* **2008**, *100*, 136406.
(47) Zhang, Y.; Yang, W. Comment on "Generalized Gradient Approximation Made Simple. *Phys. Rev. Lett.* **1998**, *80*, 890−890.
(48) VandeVondele, J.; Hutter, J. r. Gaussian Basis Sets for Accurate Calculations on Molecular Systems in Gas and Condensed Phases. *J. Chem. Phys.* **2007**, *127*, 114105.
(49) Bultinck, P.; Van Alsenoy, C.; Ayers, P.; Carbó Dorca, R. Critical Analysis and Extension of the Hirshfeld Atoms in Molecules. *J. Chem. Phys.* **2007**, *126*, 144111.
(50) Van Damme, S.; Bultinck, P.; Fias, S. Electrostatic Potentials from Self-Consistent Hirshfeld Atomic Charges. *J. Chem. Theory Comput.* **2009**, *5*, 334−340.
(51) Verstraelen, T.; Van Speybroeck, V.; Waroquier, M. The Electronegativity Equalization Method and the Split Charge Equilibration Applied to Organic Systems: Parametrization, Validation, and Comparison. *J. Chem. Phys.* **2009**, *131*, 044127.
(52) Bultinck, P.; Ayers, P.; Fias, S.; Tiels, K.; Van Alsenoy, C. Uniqueness and Basis Set Dependence of Iterative Hirshfeld Charges. *Chem. Phys. Lett.* **2007**, *444*, 205−208.
(53) Verstraelen, T.; Verstraelen, P. W.; Ayers, V.; Van Speybroeck, M.; Waroquier. The Conformational Sensitivity of Iterative Stockholder Partitioning Schemes. *Chem. Phys. Lett.* **2012**, *545*, 138−143.
(54) Verstraelen, T.; Boguslawski, K.; Tecmer, P. H.-Z. F.; Chan, M.; Kim, T. D.; Zhao, Y.; Vandenbrande, S.; Yang, D.; Gonzalez, C. E.; et al. Horton 1.2.1, http://theochem.github.com/horton/, 2013; access date: 16 September, 2015.
(55) Bussi, G.; Donadio, D.; Parrinello, M. Canonical Sampling through Velocity Rescaling. *J. Chem. Phys.* **2007**, *126*, 014101.
(56) Nose, S. A Unified Formulation of the Constant Temperature Molecular Dynamics Methods. *J. Chem. Phys.* **1984**, *81*, 511−519.
(57) Verstraelen, T.; Van Houteghem, M.; Van Speybroeck, V.; Waroquier, M. Md-Tracks: A Productive Solution for the Advanced Analysis of Molecular Dynamics and Monte Carlo Simulations. *J. Chem. Inf. Model.* **2008**, *48*, 2414−2424.
(58) Wragg, D.; Morris, R.; Burton, A. Pure Silica Zeolite-Type Frameworks: A Structural Analysis. *Chem. Mater.* **2008**, *20*, 1561−1570.
(59) Giamello, E.; Murphy, D.; Magnacca, G.; Morterra, C.; Shioya, Y.; Nomura, T.; Anpo, M. The Interaction of NO with Copper Ions in ZSM5: An EPR and IR Investigation. *J. Catal.* **1992**, *136*, 510−520.
(60) Mingos, D. M. P. *Nitrosyl Complexes in Inorganic Chemistry, Biochemistry and Medicine I*; Springer-Verlag: Berlin, 2014.
(61) De Wispelaere, K.; Ensing, B.; Ghysels, A.; Meijer, E. J.; Van Speybroeck, V. Complex Reaction Environments and Competing Reaction Mechanisms in Zeolite Catalysis: Insights from Advanced Molecular Dynamics. *Chem. - Eur. J.* **2015**, *21*, 9385−9396.
(62) Deka, U.; Lezcano-Gonzalez, I.; Warrender, S. J.; Lorena Picone, A.; Wright, P. A.; Weckhuysen, B. M.; Beale, A. M. Changing Active Sites in Cu−CHA Catalysts: DeNOx Selectivity as a Function of the Preparation Method. *Microporous Mesoporous Mater.* **2013**, *166*, 144−152.
(63) Kispersky, V.; Kropf, A. J.; Ribeiro, F.; Miller, J. Low Absorption Vitreous Carbon Reactors for Operandoxas: A Case Study on Cu/Zeolites for Selective Catalytic Reduction of NOx by NH3. *Phys. Chem. Chem. Phys.* **2012**, *14*, 2229−2238.
(64) Groothaert, M.; van Bokhoven, J.; Battiston, A.; Weckhuysen, B.; Schoonheydt, R. Bis(M-Oxo)Dicopper in Cu-ZSM-5 and Its Role in the Decomposition of NO: A Combined In Situ XAFS, UV−Vis−Near-IR, and Kinetic Study. *J. Am. Chem. Soc.* **2003**, *125*, 7629−7640.
(65) Mesu, J. G.; Mesu, T.; Visser, F.; Soulimani, E.; van Faassen, P.; de Peinder, A.; Beale, A. M.; Weckhuysen, B. M. New Insights into the Coordination Chemistry and Molecular Structure of Copper(II) Histidine Complexes in Aqueous Solutions. *Inorg. Chem.* **2006**, *45*, 1960−1971.
(66) Frank, P.; Benfatto, M.; Hedman, B.; Hodgson, K. Solution [Cu(Amm)]2+Is a Strongly Solvated Square Pyramid: A Full Account of the Copper K-Edge Xas Spectrum within Single-Electron Theory. *Inorg. Chem.* **2008**, *47*, 4126−4139.
(67) Chaboy, J.; Muñoz Páez, A.; Carrera, F.; Merkling, P.; Marcos, E. Ab Initiox-Ray Absorption Study of Copper K-Edge Xanes Spectra in Cu(Ii) Compounds. *Phys. Rev. B: Condens. Matter Mater. Phys.* **2005**, *71*, 134208.
(68) Pulido, A.; Nachtigall, P. Theoretical Investigation of Dinitrosyl Complexes in Cu-Zeolites as Intermediates in Denox Process. *Phys. Chem. Chem. Phys.* **2009**, *11*, 1447−1458.

DOI: 10.1021/acs.jpcc.5b06875
J. Phys. Chem. C 2015, 119, 24393−24403